



A highly stable neutral viologen/bromine aqueous flow battery with high energy and power density†

Cite this: *Chem. Commun.*, 2019, 55, 4801

Received 30th January 2019,
Accepted 27th March 2019

DOI: 10.1039/c9cc00840c

rsc.li/chemcomm

Wanqiu Liu,^{‡,ab} Yun Liu,^{‡,ab} Huamin Zhang,^{id ac} Congxin Xie,^{ab} Lei Shi,^{id ad}
Yong-Gui Zhou^{id ad} and Xianfeng Li^{id *ac}

An ultra-high voltage viologen/Br₂ flow battery was designed based on a novel two-electron viologen derivative, a highly-conductive and low-cost porous polyolefin membrane, and an effective complexing agent, making the battery one of the most stable two-electron viologen-based flow batteries with superior energy and power density at the same time.

The share of renewable energies in energy consumption increases globally every year due to the critical issues of environmental pollution and fossil fuel shortage. And energy storage technology is in high demand to solve the intermittency and randomness problems of renewable energies.¹ Among different technologies, flow batteries (FBs) are one of the most promising candidates to solve these problems, due to their attractive features like long cycle life, high safety, high energy efficiency, independence of energy and power ratings and environmental benignity.²

Currently, some of the FBs like vanadium flow batteries (VFBs) and Zn/Br₂ flow batteries are at a commercial demonstration stage.^{3,4} However, the relatively low energy density and high cost of these FBs hinder their commercialization.⁵ Therefore, FBs with high energy density and low cost are in urgent need.⁶ Over the last few years, various FB chemistries, from aqueous to non-aqueous, have been designed and investigated.² Non-aqueous FBs can provide a wider potential window, since the side reactions like hydrogen and oxygen evolution can be avoided. However, the low solubilities of redox couples, and low ion conductivity of electrolytes in particular, limit their energy density and power density.⁷ Aqueous FBs have advantages of high power density and high safety, making them more competitive for large-scale energy

storage.⁸ Therefore, plenty of aqueous FBs with new chemistries have been proposed and investigated. For instance, zinc-based FBs (Zn/Fe, Zn/I₂ *etc.*) have been widely investigated due to their advantages of low cost and high energy density.^{5,8} However, inorganic anolytes still pose some challenges, like the dendrite problem of zinc-based FBs. Furthermore, the solubility and stability of inorganic active materials are restricted, making it hard to further improve the battery performance. Organic anolytes, possessing many advantages like their diversity and adjustable properties, are becoming more and more attractive for FBs.⁷ Aziz *et al.* proposed a quinone/Br₂ FB, which showed a relatively high power density.⁹ However, the relatively low cell voltage (*ca.* 0.9 V) limits its application. An alkaline quinone/Fe FB increases the cell voltage to 1.2 V, but the relatively low solubility and stability of K₄Fe(CN)₆ becomes another challenge.¹⁰ A similar drawback occurs in alkaline FBs utilizing Fe(CN)^{3-/4-} as the catholyte such as FMN-Na (sodium salt of flavin mononucleotide)/Fe FB¹¹ and DHPS (7,8-dihydroxyphenazine-2-sulfonic acid)/Fe FB.¹²

Therefore, it is crucial to establish a novel aqueous FB with both highly soluble positive and negative redox couples, high cell voltage, high power density, and low cost. Methyl viologen (MV) can deliver two single-electron reductions under neutral conditions at -0.45 V and -0.76 V (*vs.* NHE), becoming one of the most promising negative redox couples for FBs, lithium ion batteries and super-capacitors.¹³⁻¹⁵ However, the insolubility of the charge-neutral state (MV⁰) in aqueous solution makes the second reduction reaction unavailable to be utilized in the battery charge and discharge process.¹³ To make use of the second reduction reaction, thereby boosting the energy density of the flow battery, Liu *et al.* proposed different chemistries by introducing functional groups in MV⁰ to improve its solubility.^{13,16} However, with the anion exchange membrane (AEM) as a separator, these FBs displayed a relatively low performance (EE < 63% at 60 mA cm⁻², Table S1, ESI†) due to the low ion conductivity of the anion exchange membrane in a neutral medium, resulting in a low power density. Besides, the high solubility of viologen derivatives with two electron reactions requires a higher solubility of the positive redox couple to maximize the energy density,

^a Dalian Institute of Chemical Physics, Chinese Academy of Sciences, 457 Zhongshan Road, Dalian 116023, P. R. China. E-mail: lixianfeng@dicp.ac.cn

^b University of Chinese Academy of Sciences, Beijing 100039, P. R. China

^c Collaborative Innovation Center of Chemistry for Energy Materials (iChEM), Dalian 116023, P. R. China

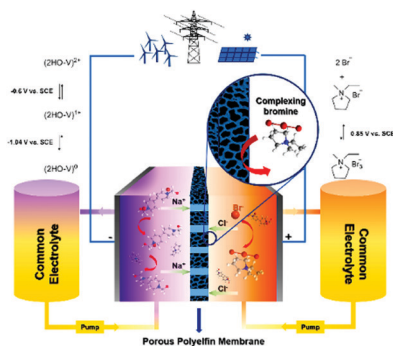
^d State Key Laboratory of Catalysis, Dalian Institute of Chemical Physics, Chinese Academy of Sciences, Zhongshan Road 457, Dalian 116023, China

† Electronic supplementary information (ESI) available. See DOI: 10.1039/c9cc00840c

‡ These authors contributed equally to this article.

which means a concentration of 2.2 M viologen derivatives needs a concentration of at least 4.4 M positive active material. And the most of the reported organic positive active material cannot meet the requirement of such a high solubility. In addition, the instability of a viologen based battery is one of the critical challenges due to the irreversible crossover of redox couples. The Br_2/Br^- redox couple, which possesses the advantages of a very high solubility (up to 29 M), a very high potential (0.85 V vs. SCE) and high reversibility, is a kind of very promising cathode material for high energy density FBs. However, the FBs of viologen based anodes and Br_2 cathodes are rarely reported, due to some critical challenges. One of the challenges is that the complexation reaction between Br_2 and viologen can produce a solid precipitate and further terminate the cycle life. The second arises from the Br_2 shuttle from the cathode to the anode, which greatly decreases the stability of these batteries as well.

Herein, we report a neutral (1,1'-di(2-ethanol)-4,4'-bipyridinium dibromide ((2HO-V) Br_2)/ Br_2 FB with a superior high cell voltage (1.49 V and 1.89 V) and high energy density (theoretical energy density is 95.1 W h L^{-1}) and power density (Scheme 1). For the negative side, homemade (2HO-V) Br_2 was used, in which a hydroxyl group was introduced into a viologen molecule to increase the solubility of the charge-zero state in water from <10 mM to more than 2 M.¹³ For the positive side, a Br^-/Br_2 redox couple was utilized as the positive redox couple due to the high solubility of Br^- and Br_3^- , and its high potential and excellent electrochemical properties.¹⁷ In addition, a complexing agent of Br_3^- , 1-ethyl-1-methylpyrrolidinium bromide (MEP), was introduced to prevent the complexation of (2HO-V) Br_2 and Br_2 , and therefore increase the stability of the battery. Meanwhile, by the complexation of Br_2 with MEP, a porous polyolefin membrane of a much lower cost could be used to separate the MEP- Br_2 complexation of a relatively large size by pore size exclusion. And the membrane can provide a much higher ion conductivity under neutral conditions, and thereby a much higher power density. Consequently, the assembled (2HO-V) Br_2 / Br_2 FB could operate with an energy efficiency of 90.3% at 20 mA cm^{-2} and 83.4% at 40 mA cm^{-2} . Furthermore, the battery with a higher-concentration electrolyte was also evaluated, obtaining an EE of about 74% for a battery with 1.0 M (2HO-V) Br_2 in the anolyte. Most importantly, using bromide viologen allowed a common electrolyte (2HO-V) Br_2 at both sides, which can effectively solve the critical issues arising from the redox crossover. And finally a highly stable (2HO-V) Br_2 FB with a two-electron reaction can be created.



Scheme 1 Representation of the FB and its anodic and cathodic half-cell reactions.

The working principle of the neutral (2HO-V) Br_2 / Br_2 FB is illustrated in Fig. 1. According to the theory of molecular design engineering, the introduction of a hydrophilic group can increase the solubility of the molecule, while the addition of an electro-donating group can decrease the redox potential of the molecule. To this end, we chose the hydroxyl group ($-\text{OH}$) as a substituent because of its high hydrophilicity, as well as the strong electron-donating effect. The designed molecule, (2HO-V) Br_2 , was prepared by a very simple one-step method (Fig. 1a), which is very easy for upscaling. The structure and purity of (2HO-V) Br_2 were characterized by ^1H NMR (Fig. S1, ESI †). As expected, the solubility of (2HO-V) Br_2 and its charge-zero state can reach 2.2 M and 2.1 M in H_2O , respectively. Considering its ability to store two electrons per molecule, this solubility corresponds to a charge capacity of 112.6 A h L^{-1} . When paired with the Br^-/Br_2 redox couple, as shown in Fig. 1b, the battery would have an ultrahigh cell voltage of 1.49 V for the first reduction and 1.89 V for the second reduction, equivalent to the theoretical energy density of up to 95.1 W h L^{-1} . The reaction of the (2HO-V) Br_2 in the anolyte during the charge and discharge process is shown in Fig. 1c.

Detailed analysis of the electrochemical properties of (2HO-V) Br_2 was performed by cyclic voltammetry (CV) at different sweep rates from 10 mV s^{-1} to 200 mV s^{-1} using a glassy carbon as the working electrode and a graphite electrode as the counter electrode (Fig. S4a, ESI †). The results showed that both redox couples (2HO-V) $^{2+/1+}$ and (2HO-V) $^{1+/0}$ were fully reversible, confirming the solubility of the charge-zero state (2HO-V) 0 .¹³ The two redox potentials of (2HO-V) Br_2 were observed at -0.64 V and -1.04 V versus the saturated calomel electrode (SCE). The second redox potential decreases due to the introduction of the $-\text{OH}$ group. Besides, the peak currents of these two reductions showed a linear relationship with the square root of scan rate ($\nu^{1/2}$, Fig. S4b, ESI †), indicating that both redox couples of (2HO-V) $^{2+/1+}$ and (2HO-V) $^{1+/0}$ were reversible and diffusion controlled. To further investigate the electrochemical kinetics of the (2HO-V) Br_2 , the diffusion coefficient was measured by linear sweep voltammetry (LSV) using a glassy carbon rotating disk electrode (Fig. S4d, ESI †). The second and third plateaus observed in the LSV curves corresponded to the first and second single-electron reduction of (2HO-V) Br_2 , while the first plateau might be due to the surface adsorption of the (2HO-V) Br_2 molecule. Levich analysis was performed to calculate the diffusion coefficient which was 5.19×10^{-6} $\text{cm}^2 \text{s}^{-1}$ and 3.99×10^{-6} $\text{cm}^2 \text{s}^{-1}$ for the first and

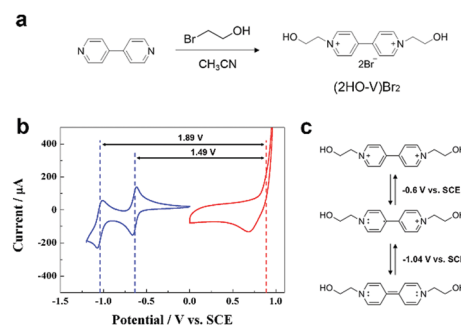


Fig. 1 (a) Synthesis of (2HO-V) Br_2 . (b) Cyclic voltammograms of 4 mM (2HO-V) Br_2 (-0.64 V and -1.04 V vs. SCE) and 10 mM KBr (0.85 V vs. SCE) in 1 M NaCl solution, respectively. (c) Reaction mechanism of (2HO-V) Br_2 in the FB.

second electron reduction, respectively (Fig. S4e, ESI†). We also estimated the rate constants (k^0) for the electron transfer of $(2\text{HO-V})\text{Br}_2$ by the Nicholson's method. The results showed that the k^0 was $>0.356 \text{ cm s}^{-1}$ for the first reduction and $>0.312 \text{ cm s}^{-1}$ for the second reduction, indicating a very fast electron transfer. Combining the high solubility, good electrochemical reversibility and fast electron transfer, the $(2\text{HO-V})\text{Br}_2$ is expected to be an excellent anolyte for FBs.

To qualify the two-electron storage capability of $(2\text{HO-V})\text{Br}_2$, KBr was chosen as the catholyte for its high solubility in H_2O ($>5.4 \text{ M}$ in H_2O , 20°C) and the high redox potential of Br_2/Br^- (0.85 V vs. SCE). Br_2/Br^- has been widely used in FBs such as Zn/Br_2 FB and exhibits excellent battery performances. However, Br_2 can coordinate with the $(2\text{HO-V})\text{Br}_2$ and form an insoluble complex ($^1\text{H NMR}$ spectrum of the precipitate is shown in Fig. S2, ESI†).²¹ This insoluble complex can not only reduce the utilization of Br_2 , but also block the pores of the membrane, causing an increased resistance of the membrane and a decreased battery performance. To solve this problem, a Br_2 complexing agent with a higher binding energy associated with the formation of the complex than that of $(2\text{HO-V})\text{Br}_2$ was added to electrolytes. Density functional theory (DFT) modelling of the binding energy of the Br_2 complexing agent (MEP), and $(2\text{HO-V})\text{Br}_2$ with Br_2 was done to find whether it can complex with the Br_2 and thus inhibit the formation of precipitate. The DFT energy-minimized structures of the two complexes are shown in Fig. 2. Calculations for the binding energy of MEP- Br_2 and $(2\text{HO-V})\text{Br}_2$ - Br_2 were performed using the Gaussian 09 package. In order to simplify the calculation, the $(2\text{HO-V})^{2+}$ was only modelled as one half, considering its symmetric structure. The calculated values of binding energy are summarized in the ESI† (Table S2). The results showed that the binding energy of MEP and Br_2 was much higher than that of $(2\text{HO-V})\text{Br}_2$, indicating that the Br_2 molecule tends to coordinate with MEP rather than with $(2\text{HO-V})\text{Br}_2$. These results could be explained by the fact that the N^+ on the MEP are more positively charged, while the electrons on the $(2\text{HO-V})^{2+}$ are more evenly distributed due to the influence of the benzene ring. Therefore, MEP can suppress the precipitation of the $(2\text{HO-V})\text{Br}_2$ - Br_2 complex and increase the stability of $(2\text{HO-V})\text{Br}_2/\text{Br}_2$ FB. Meanwhile, by the complexation of MEP and Br^{3-} , the permeability of Br^{3-} can also be greatly reduced according to the permeability tests of Br^{3-} and MEP- Br^{3-} (Fig. S8, ESI†).

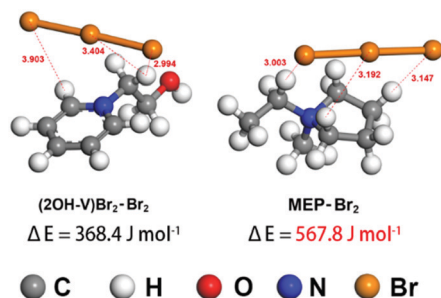


Fig. 2 Theoretical calculations of binding energies.

By using MEP as the Br_2 complexing agent in the catholyte and a porous polyolefin membrane with high ion conductivity and low cost as the separator, a FB was constructed using 0.2 M $(2\text{HO-V})\text{Br}_2$ and 1.2 M KBr in a 2.0 M NaCl supporting electrolyte for the anolyte and catholyte, respectively. The assembled battery exhibited an optimal performance with a coulombic efficiency (CE) of 99.8% and an EE of 83.4% at 40 mA cm^{-2} . This high EE is an indication of a very high power density. The rate performance was investigated as shown in Fig. 3a. The CE was nearly 100% from 20 mA cm^{-2} to 100 mA cm^{-2} , while the EE decreased from 90.3% to 67.4% due to the increased electrochemical polarization and ohmic polarization. In addition, the battery could continuously operate for more than 100 cycles with no obvious efficiency fading (Fig. 3b). A representative voltage profile is shown in the inset of Fig. 3b. Fig. 3c shows the rate performance of the battery with 0.5 M $(2\text{HO-V})\text{Br}_2$. The CE increases from 98.0% to 99.9% as the current density increases from 20 mA cm^{-2} to 80 mA cm^{-2} . However, the EE decreases from 86.6% to 68.5%. With an increase in concentration, the discharge capacity increases from 10.0 A h L^{-1} to 25.6 A h L^{-1} , and the discharge energy density increases from 14.0 W h L^{-1} to 36.4 W h L^{-1} . The cycling performance of the battery with 0.5 M $(2\text{HO-V})\text{Br}_2$ showed very slight efficiency decay over 50 cycles (Fig. S5, ESI†). To further improve the energy density, we evaluated the battery with a higher-concentration electrolyte. As shown in Fig. 3d, even with 1.0 M $(2\text{HO-V})\text{Br}_2$ in the anolyte, the battery could achieve an energy efficiency of about 74% at a current density of 40 mA cm^{-2} .

However, the crossover of redox couples between different anolytes and catholytes resulted in a fast capacity decay during the cycling (Fig. S6, ESI†), which is one of the most troublesome issues with FBs. To solve this problem, a common electrolyte was used to alleviate the crossover of redox couples and enhance the cycling performance of batteries. Because of the effective

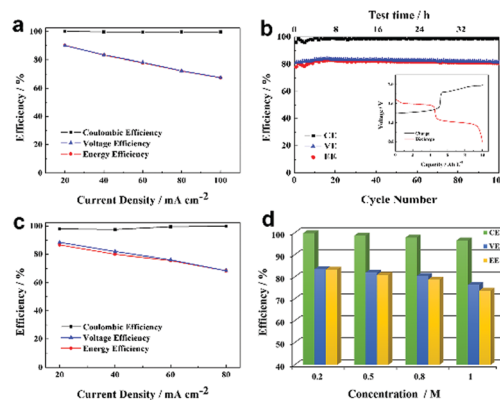


Fig. 3 (a) Plot of average CE, EE and voltage efficiency (VE) at different current densities from 20 to 100 mA cm^{-2} . (b) Cycling performance of the assembled FB at a current density of 40 mA cm^{-2} ; inset: representative charge and discharge curves from the experiment. Conditions: anolyte: 0.2 M $(2\text{HO-V})\text{Br}_2$ in 2 M NaCl; catholyte: 1.2 M KBr and 0.8 M MEP in 2 M NaCl. (c) Plot of average CE, EE and VE at different current densities from 20 to 80 mA cm^{-2} . Conditions: anolyte: 0.5 M $(2\text{HO-V})\text{Br}_2$ in 2 M NaCl; catholyte: 1.2 M KBr and 0.4 M MEP in 2 M NaCl. (d) Plot of average CE, EE and VE at different concentrations of 0.2 M , 0.5 M , 0.8 M and 1 M $(2\text{HO-V})\text{Br}_2$ at a current density of 40 mA cm^{-2} .

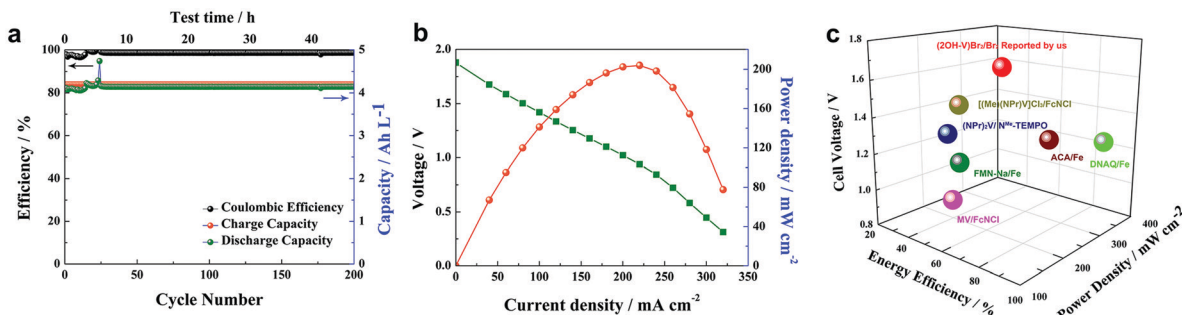


Fig. 4 (a) Cycling performance of the assembled FB with a common electrolyte at a current density of 40 mA cm^{-2} . Conditions: both anolyte and catholyte: $0.1 \text{ M (2HO-V)Br}_2$, 0.4 M MEP and 0.6 M KBr in 2 M NaCl . (b) Polarization and power density curves of the $(2\text{HO-V})\text{Br}_2/\text{Br}_2$ FB at 80% SOC. (c) Cell voltage, power density and energy efficiency of the $(2\text{HO-V})\text{Br}_2/\text{Br}_2$ FB and other aqueous organic FBs.^{10,11,16,18–20}

inhibition of the $(2\text{HO-V})\text{Br}_2\text{-Br}_2$ complex precipitation by MEP, the flow battery with a common electrolyte bromine viologen could operate steadily. As a result, the $(2\text{HO-V})\text{Br}_2/\text{Br}_2$ FB demonstrated a very stable cycling performance at a current density of 40 mA cm^{-2} with no obvious capacity decay in 200 cycles (Fig. 4a and Fig. S7, ESI[†]). The UV-vis absorption spectrum of the anolyte after 70 cycles was detected (Fig. S9, ESI[†]). Due to the similar UV absorption peak position of $(2\text{HO-V})\text{Br}_2$ and Br^{3-} , the peak intensity after the battery cycles slightly increased. In the polarization test at 80% state of charge (SOC), the $(2\text{HO-V})\text{Br}_2/\text{Br}_2$ FB can achieve 204 mW cm^{-2} of peak power density, which is one of the highest power densities of neutral FBs (Fig. 4b). Compared with most reported systems, our $(2\text{HO-V})\text{Br}_2/\text{Br}_2$ FB shows tremendous advantages in cell voltage, power density and energy efficiency, as shown in Fig. 4c. Both the cell voltage and EE of our $(2\text{HO-V})\text{Br}_2/\text{Br}_2$ FB are the highest among the reported viologen-based FBs.

In summary, we have developed a highly stable $(2\text{HO-V})\text{Br}_2/\text{Br}_2$ FB that achieves high energy and power density. By introducing a hydrophilic and an electron-donating $-\text{OH}$ group into a viologen molecule, the $(2\text{HO-V})\text{Br}_2$ can provide two single-electron reactions and a highly negative potential. Using highly soluble Br_2/Br^- as a positive redox couple enables an ultra-high cell voltage, and a further high energy density (95.1 W h L^{-1}) of the battery. Adding a complexing agent MEP can prevent the precipitation of the $(2\text{HO-V})\text{Br}_2\text{-Br}_2$ complex, ensuring a steady operation of the FB. Besides, upon the complexation of Br_2 and the MEP molecule, the size of Br_2 increases. Hence, a porous polyolefin membrane can be used in this FB. Employing the porous polyolefin membrane with a low-cost and high ion conductivity enables the battery to operate at a high current density of 100 mA cm^{-2} and achieve a high energy efficiency of 83.4% at a current density of 40 mA cm^{-2} . Most importantly, a common electrolyte, bromide viologen, can be used to greatly improve the capacity retention. As a result, the battery with the common electrolyte can run continuously for more than 200 cycles with no capacity decay. The battery performance of this neutral $(2\text{HO-V})\text{Br}_2/\text{Br}_2$ FB can be further promoted by adjusting the concentration of MEP, changing the supporting electrolyte and tuning the thickness of the porous polyolefin membrane. Therefore, this neutral $(2\text{HO-V})\text{Br}_2/\text{Br}_2$ FB with a high energy density, power density and low cost is a very promising and sustainable energy storage device.

The authors acknowledge financial support from CAS-DOE program, the Dalian Science and Technology Innovation Project (2018J12GX050) and DICP funding (ZZBS201707).

Conflicts of interest

There are no conflicts to declare.

Notes and references

- W. Wang, Q. Luo, B. Li, X. Wei, L. Li and Z. Yang, *Adv. Funct. Mater.*, 2013, **23**, 970–986.
- W. Liu, W. Lu, H. Zhang and X. Li, *Chem. – Eur. J.*, 2019, **25**, 1649–1664.
- C. Wang, Q. Lai, P. Xu, D. Zheng, X. Li and H. Zhang, *Adv. Mater.*, 2017, **29**, 1605815.
- G. Kear, A. A. Shah and F. C. Walsh, *Int. J. Energy Res.*, 2012, **36**, 1105–1120.
- C. Xie, H. Zhang, W. Xu, W. Wang and X. Li, *Angew. Chem., Int. Ed.*, 2018, **57**, 1–7.
- C. Minke and T. Turek, *J. Power Sources*, 2018, **376**, 66–81.
- Y. Ding, C. Zhang, L. Zhang, Y. Zhou and G. Yu, *Chem. Soc. Rev.*, 2018, **47**, 69–103.
- C. Xie, Y. Duan, W. Xu, H. Zhang and X. Li, *Angew. Chem., Int. Ed.*, 2017, **56**, 14953–14957.
- B. Huskinson, M. P. Marshak, C. Suh, S. Er, M. R. Gerhardt, C. J. Galvin, X. Chen, A. Aspuru-Guzik, R. G. Gordon and M. J. Aziz, *Nature*, 2014, **505**, 195–198.
- Q. Chen, K. Lin, M. R. Gerhardt, L. Tong, S. B. Kim, A. W. Valle, L. Eisenach, D. Hardee, R. G. Gordon, M. P. Marshak and M. J. Aziz, *Science*, 2015, **349**, 1529–1532.
- A. Orita, M. G. Verde, M. Sakai and Y. S. Meng, *Nat. Commun.*, 2016, **7**, 13230.
- A. Hollas, X. Wei, V. Murugesan, Z. Nie, B. Li, D. Reed, J. Liu, V. Sprenkle and W. Wang, *Nat. Energy*, 2018, **3**, 508–514.
- J. Luo, B. Hu, C. Debruler and T. L. Liu, *Angew. Chem., Int. Ed.*, 2018, **57**, 231–235.
- B. Evanko, S. J. Yoo, S. E. Chun, X. Wang, X. Ji, S. W. Boettcher and G. D. Stucky, *J. Am. Chem. Soc.*, 2016, **138**, 9373–9376.
- S. J. Yoo, B. Evanko, X. Wang, M. Romelczyk, A. Taylor, X. Ji, S. W. Boettcher and G. D. Stucky, *J. Am. Chem. Soc.*, 2017, **139**, 9985–9993.
- C. DeBruler, B. Hu, J. Moss, X. Liu, J. Luo, Y. Sun and T. L. Liu, *Chem*, 2017, **3**, 961–978.
- Q. Lai, H. Zhang, X. Li, L. Zhang and Y. Cheng, *J. Power Sources*, 2013, **235**, 1–4.
- M. E. Easton, A. J. Ward, B. Chan, L. Radom, A. F. Masters and T. Maschmeyer, *Phys. Chem. Chem. Phys.*, 2016, **18**, 7251–7260.
- T. Liu, X. Wei, Z. Nie, V. Sprenkle and W. Wang, *Adv. Energy Mater.*, 2016, **6**, 1501449.
- B. Hu, C. DeBruler, Z. Rhodes and T. L. Liu, *J. Am. Chem. Soc.*, 2017, **139**, 1207–1214.
- B. Hu, Y. Tang, J. Luo, G. Grove, Y. Guo and T. L. Liu, *Chem. Commun.*, 2018, **54**, 6871–6874.